

Identification and expression analysis of xyloglucan endotransglucosylase/hydrolase (XTH) family in grapevine (*Vitis vinifera* L.)

Tian Qiao^{1,*}, Lei Zhang^{1,*}, Yanyan Yu¹, Yunning Pang¹, Xinjie Tang¹, Xiao Wang¹, Lijian Li¹, Bo Li² and Qinghua Sun¹

¹State Key Laboratory of Crop Biology, College of Life Science, Shandong Agricultural University, Taian, Shandong, China

²Shandong Academy of Grape, Shandong Academy of Agricultural Sciences, Jinan, Shandong, China

* These authors contributed equally to this work.

ABSTRACT

Xyloglucan endotransglucosylases/hydrolases (XTH) are key enzymes in cell wall reformulation. They have the dual functions of catalyzing xyloglucan endotransglucosylase (XET) and xyloglucan endonuclease (XEH) activity and play a crucial role in the responses against abiotic stresses, such as drought, salinity, and freezing. However, a comprehensive analysis of the XTH family and its functions in grapevine (*Vitis vinifera* L.) has not yet been completed. In this study, 34 XTHs were identified in the whole grapevine genome and then named according to their distribution on chromosomes. Based on a phylogenetic analysis including *Arabidopsis* XTHs, the VvXTHs were classified into three groups. Cis-element analysis indicated that these family members are related to most abiotic stresses. We further selected 14 VvXTHs from different groups and then examined their transcription levels under drought and salt stress. The results indicated that the transcription levels of selected VvXTHs in the leaves and roots presented the largest changes, suggesting that VvXTHs are likely to take part in the responses to drought and salt stress in grapevines. These results provide useful evidence for the further investigation of VvXTHs function in response to abiotic stresses in grapevine.

Submitted 4 January 2022

Accepted 16 May 2022

Published 13 June 2022

Corresponding authors

Bo Li, sdtalibo@163.com

Qinghua Sun, qhsun@sdaa.edu.cn

Academic editor

Kashmir Singh

Additional Information and
Declarations can be found on
page 17

DOI 10.7717/peerj.13546

© Copyright

2022 Qiao et al.

Distributed under

Creative Commons CC-BY 4.0

OPEN ACCESS

Subjects Agricultural Science, Molecular Biology, Plant Science

Keywords VvXTH, *Vitis vinifera*, Phylogenetic analysis, Expression pattern, Abiotic stress

INTRODUCTION

As one of the most economically fruit crops, grapevine (*Vitis vinifera* L.) is cultivated worldwide (Feng, He & Hiroto, 2000). However, the growth of grapes in natural environment is inevitably impacted by a series of abiotic stresses, including salinity, drought, and extreme temperatures, which damage the cell walls of the plants, disrupt the biofilm system, and ultimately affect the quality and yield of the fruit (Araujo, Abiodun & Crespo, 2016; Liu et al., 2019; Ning et al., 2017). Xyloglucan endotransglucosylase/hydrolase (XTH) can carry out cell wall structural modification and rearrangement by severing and repolymerizing cellulose mono-xyloglucan cross-linked

structures (Campbell & Braam, 2010). It belongs to the glycoside hydrolase 16 (GH16) family, which is a subfamily of glycoside hydrolases containing diverse enzymes with different specific targets, such as keratan sulfate, β -1,3-glucans, mixed linkage β -1,3(4)-glucans, xyloglucans, j-carrageenan, and agarose (Mark et al., 2009; Stratilova et al., 2020). All XTH proteins present the typical structure of XTH enzymes: the (D/N)E(I/L/A/V/F)(D/T)(F/I)E(F/I/L)LG motif, which includes the catalytic active-site residues ExDxE (Matsui et al., 2005; Liu et al., 2007; Miedes & Lorences, 2009; Singh et al., 2011). XTH proteins may present one or two enzyme activities: xyloglucan endonuclease (XEH) activity and/or xyloglucan endotransglucosylase (XET) activity. The former specifically hydrolyzes xyloglucan β -1,4 glycosidic bonds, cleaving the xyloglucan chain, thereby shortening the xyloglucan chain, and the latter can transfer xyloglucan fragments between xyloglucan chains, elongating xyloglucan chains (Han et al., 2016).

Thus far, the XTH family has been identified and analyzed in species such as *Arabidopsis thaliana* (33), *Hordeum vulgare* (24), *Glycine max* (61), and *Nicotiana tabacum* (54). (Nomchit et al., 2010; Li et al., 2018; Meng et al., 2018; Cheng et al., 2021; Strohmeier et al., 2004; Tiika et al., 2021). The XTH family was initially classified into three groups, named groups I, II, and III, in *Arabidopsis* (Campbell & Braam, 1999). However, a subsequent study in *Oryza sativa* found that there was no clear distinction between groups I and II; therefore, rice XTHs were divided into only two groups: group I/II and group III (Eklof & Brumer, 2010). The XTH members in group III could be further divided into two subgroups (IIIA and IIIB) according to their three-dimensional structures (Baumann et al., 2007; Fu, Liu & Wu, 2019). Moreover, a small outlier group was identified close to the root of the tree and was named the ancestral group. The XTHs of group I/II and group IIIB showed primarily or only XET activity, while the XTHs in group IIIA mainly displayed XEH activity (Eklof & Brumer, 2010; Nomchit et al., 2010; Opazo et al., 2017). Further studies revealed that each type of enzyme activity was determined by several structural characteristics. For example, in the protein structure of *TmNXG1*, loop two is the key structure affecting hydrolysis and transglycosylase activity (Mark et al., 2009). *PttXET16-34* contained an important N-glycan structure, which is found in all group I/II members but absent in almost all IIIA groups (such as *TmNXG1*). Interestingly, the N-glycosylation site shifts from the C-terminus to the other side of the active-site cleft in group IIIB (Mark et al., 2009; Eklof & Brumer, 2010).

Increasing evidence has revealed that XTHs are instrumental for coping with abiotic stresses through cell remodeling and enhanced cell wall biogenesis in plants (Eklof & Brumer, 2010; Tiika et al., 2021). For instance, the constitutive expression of *CaXTH3* has been verified to enhance resistance to salinity and drought stress in tomato plants (Choi et al., 2011). *AtXTH11*, *AtXTH29*, and *AtXTH33* were observed to be upregulated through different secretory pathways in *Arabidopsis* seedlings treated with heat stress and drought stress (Caroli, Manno & Lenucci, 2021). A recent study revealed that the overexpression of persimmon *DkXTH1* promotes tolerance to salt and drought stress by improving photosynthesis and reducing lipid peroxidation (Han et al., 2017). Additionally, transgenic tobacco with estradiol-inducible expression of *SIXTH10* shows stronger growth under salinization and hypothermia conditions (Norbert et al., 2020), and

GmXTH expression levels have been reported to be significantly associated with flooding stress (Li et al., 2018). Transgenic soybeans overexpressing *AtXTH31* also exhibit increased tolerance to flooding stress (Li et al., 2018). Moreover, an *AtXTH19* mutant was demonstrated to show lower freezing tolerance during cold and subzero acclimation than the wild type, which is likely related to differences in the cell wall composition and structure (Daisuke et al., 2020).

Taken together, the above studies highlight the essential functions of *XTHs* in resisting abiotic stress. In fact, the identification of novel genes involved in abiotic stress resistance and their application in genetic breeding is now considered an effective approach for the improvement of stress resistance in grapes. The existence of a high-quality *de novo*-assembled grape genome has made it possible to identify gene families in this species. In this study, we isolated and identified the *XTH* family members from grapevine and performed a complete bioinformatics analysis of the *XTH* family. Interestingly, we identified some putative members with potential functions under abiotic stresses, especially salt and drought stress. These findings allow in-depth research on the potential functions of the selected *VvXTHs* in grapevine.

MATERIALS AND METHODS

Identification and biochemical analysis of *XTHs* in grapevine

The sequence annotations of the whole genome and the gene GFF3 file were downloaded by using CRIBI v2.1 (<https://urgi.versailles.inra.fr/Species/Vitis/Annotations>) (Canaguier et al., 2017). We also downloaded hidden Markov models (PF00722 and PF06958) of the *XTH* domain from the Pfam database (<http://pfam.xfam.org>) and obtained the candidate gene sequence numbers of the grapevine *XTH* family with HMMer software (Potter et al., 2018). To avoid duplication and the inclusion of sequences without *XTH* family domain characteristics, sequences without the *XTH* domain and sequences showing alternative splicing were removed. The EMBL-EBI online tool (<http://pfam.xfam.org/search/sequence>) (Gaia et al., 2021) was used to further analyze secondary structure domains, and the sequences without typical *XTH* domains were removed.

The relative molecular weight (MW), hydrophilicity (GRAVY), and isoelectric point (pI) of these *VvXTHs* were predicted and analyzed using Expasy (<https://www.expasy.org/>) (Duvaud et al., 2021). Single peptide (SP) prediction was performed on the SignalP v4.1 server (<https://services.healthtech.dtu.dk/service.php?SignalP-5.0>).

Gene structures were analyzed with Gene Structure Display Server software (<http://gsds.gao-lab.org/>) (Hu et al., 2015). Conserved motifs in *VvXTHs* were statistically identified with the online Multiple EM for Motif Elicitation (MEME) software (<https://meme-suite.org/meme/tools/meme>) (Bailey et al., 2009), and TBtools was then used for the clustering and visualization of *VvXTHs* in grapevine. Multiple protein sequence alignments were performed with ClustalX software and the Esript 3.0 online program (<https://esript.ibcp.fr/ESPrpt/ESPrpt/>) (Larkin et al., 2007).

Phylogenetic analysis of VvXTHs in grapevine

To investigate the phylogenetic relationship of VvXTHs, the 34 VvXTH protein sequences from grapevine and the 33 AtXTH protein sequences from *Arabidopsis* were used for multiple sequence alignment by using the Clustal W program within MEGA 11.0 software (Sudhir *et al.*, 2018). The phylogenetic tree was built using the neighbor-joining (NJ) method with 1,000 bootstrap replications and the p-distance model and was then validated by the maximum likelihood method. To better visualize the phylogenetic tree, the final tree diagram file (*.nwk) was uploaded from MEGA to Figtree and EVOLVIEW online software (<http://www.evolgenius.info/evolview/>) (Balakrishnan *et al.*, 2019).

The Grape Genome Browser (12X) (<http://www.genoscope.cns.fr/externe/GenomeBrowser/Vitis/>) provided chromosomal location data for all VvXTHs. We used TBtools to identify and illustrate the distribution of genes on chromosomes. MCScanX with the default parameters was applied to identify gene duplication events. The CIRCOS program (<https://github.com/CJ-Chen/TBtools>) was used to analyze syntenic relationships among VvXTHs. VvXTHs falling within the identified collinear blocks were regarded as segmental events, and any two genes separated by a distance of less than 100 KB whose similarity exceeded 75% were considered tandem duplications. To visualize the synteny relationships of orthologous XTHs derived from grapes and *Arabidopsis*, Dual Synteny Plotter software (<https://github.com/CJ-Chen/TBtools>) was applied to construct a syntenic analysis map (Xie *et al.*, 2018). The *Arabidopsis* sequences were obtained from The *Arabidopsis* Information Resource (TAIR) database (<https://www.arabidopsis.org/>) (Han *et al.*, 2013). TBtools software was used to calculate the nonsynonymous (Ka) and synonymous (Ks) substitution rates and Ka/Ks ratio of each gene pair. Divergence times were calculated as follows: $T = Ks/2\lambda$ ($\lambda = 6.5 \times 10^{-9}$ for grapevine) (Li *et al.*, 2019a).

Cis-element analysis of XTHs in grapevine

The sequences within 1,500 base pairs (bp) upstream of the starting codon of the VvXTHs were obtained from Ensembl Plants (<http://plants.ensembl.org/index.html>) as the promoter regions (Dan *et al.*, 2017). The cis-elements were predicted with PlantCARE Web Tools (<http://bioinformatics.psb.ugent.be/webtools/plantcare/html/>) (Magali *et al.*, 2002) and New PLACE Web Tools (<https://www.dna.affrc.go.jp/PLACE/?action=newplace>). TBtools was used to draw heatmaps and build clustering trees.

Gene expression analysis of XTHs in different grapevine organs and tissues

To understand the spatial and temporal expression patterns of VvXTHs during development, a high-throughput microarray data, from a gene expression atlas generated from different organs/tissues at different developmental stages (Marianna *et al.*, 2012), was employed for further analysis. According to the gene ID, the expression profiles of VvXTHs was extracted from the GSE36128 data set, and we then normalized the average expression value of each gene in 54 samples (including green and woody tissues and organs at different developmental stages as well as specialized tissues such as pollen and senescent leaves). TBtools was used to draw heatmaps and build clustering trees.

To verify the reliability of the results obtained from the [GSE36128](#) data set, the organ-specific expression patterns were examined with quantitative real-time RCR (qRT-PCR) using the five different organs (tendrils, root, stem, leaf and flower) from 5-year-old trees of grapevine “Crimson” growing at the experiment station of Shandong Agricultural University (Taian, Shandong, China).

RNA extraction and expression analysis of *VvXTHs*

The tissue culture seedlings of *Vitis vinifera* cv “Crimson” seedless were grown on 1/2 Murashige and Skoog (MS) solid medium with 0.2 mM indole-3-butyric acid (IBA) under a 16-h-light/8-h dark cycle at 24 ± 1 °C for 6 weeks. Six-week-old seedlings, which transcription level changes more pronounced, were transferred to liquid medium containing 200 mM NaCl or 200 mM mannitol for salt and drought stress treatments, respectively. The treated seedlings were extracted and separated into leaves and roots for 0, 3, 6, 9, 12, and 24 h upon treatment, immediately frozen in liquid nitrogen and stored at -80 °C for RNA extraction. For each sample, three biological replicates were collected.

Total RNA was extracted from the samples treated with NaCl and mannitol using a HiPure HP Plant RNA Mini Kit (Magen, Guangzhou, China) based on the supplier’s instructions. Subsequently, first-strand cDNA was synthesized from total RNA with the PrimeScript™ RT reagent kit with gDNA Eraser (Vazyme Biotech Co., Nanjing, China). qRT-PCR was performed using a SYBR® PrimeScript™ RT-PCR Kit (TaKaRa, Dalian, China) according to the supplier’s instructions with a CFX96™ Real-Time PCR Detection System. Gene expression levels were normalized against the average expression of the internal reference gene, and the baseline and Ct (threshold cycles) value were automatically determined by the CFX Manager software program. The relative expression levels of *VvXTHs* were calculated using the $2^{-\Delta\Delta Ct}$ comparative Ct method. The internal reference gene used in this study was *Vvβ-actin7* (XM_034827164), which has been proved to be a most stable gene for normalization by comparison with other reference gene (*Vvβ-actin101*: XM_002265440) (Fig. S1). All experiments were performed with three biological replicates, and all the primers used in this study are listed in Table S1. To visualizing the relative difference, the expression level of 0 h treatments for salt and drought stresses and tendrils for plant tissue specificity was set as 1, respectively. Then, TBtools was used to draw a heatmap for visualization.

RESULTS

Identification and analysis of *VvXTHs* in grapevine

Forty-two sequences were identified by searching for two domains (Pfam: PF00722 and PF06955) with the HMMer program. We deleted six alternative splicing sequences and two sequences without typical XTH domains. As a result, we finally identified 34 *VvXTHs*. Described by previous studies ([Cao et al., 2016](#); [Fu, Liu & Wu, 2019](#); [Li et al., 2018](#); [Wan et al., 2014](#)), we named these genes according to their chromosomal locations and named them *VvXTH1-VvXTH34*.

The analysis of the physical and biochemical data of the 34 *VvXTHs*, including their amino acids (AAs), MWs, SPs, pIs, total average hydrophilicity (GRAVY) and subcellular

Table 1 Molecular characteristics of VvXTHs in grapevine.

Name	Gene identifier	AA	MW (Da)	SP	pI	GRAVY	Subcellular localization
VvXTH1	VIT_201s0011g06250	279	32,099.88	-	6.60	-0.649	Plasma membrane
VvXTH2	VIT_201s0026g00200	313	35,198.85	24	6.83	-0.296	Extracellular
VvXTH3	VIT_201s0150g00460	307	35,270.14	35	8.65	-0.366	Plasma membrane
VvXTH4	VIT_202s0012g02220	341	38,867.80	-	8.99	-0.374	Plasma membrane
VvXTH5	VIT_203s0088g00650	295	34,401.83	25	7.12	-0.372	Plasma membrane
VvXTH6	VIT_205s0062g00240	281	32,143.11	24	9.22	-0.389	Plasma membrane
VvXTH7	VIT_205s0062g00250	279	32,239.31	24	9.07	-0.449	Plasma membrane
VvXTH8	VIT_205s0062g00480	281	32,088.01	24	9.08	-0.406	Plasma membrane
VvXTH9	VIT_205s0062g00610	281	32,173.18	24	9.14	-0.408	Plasma membrane
VvXTH10	VIT_206s0061g00550	291	32,696.72	18	5.74	-0.438	Extracellular
VvXTH11	VIT_207s0185g00050	280	32,102.92	19	7.11	-0.555	Plasma membrane
VvXTH12	VIT_208s0007g04950	293	33,761.16	18	9.45	-0.457	Extracellular
VvXTH13	VIT_210s0116g00520	300	34,816.90	27	4.61	-0.584	Plasma membrane
VvXTH14	VIT_210s0003g02440	294	33,673.17	27	9.44	-0.375	Plasma membrane
VvXTH15	VIT_210s0003g02480	290	32,860.23	27	8.18	-0.278	Plasma membrane
VvXTH16	VIT_211s0016g03480	291	33,246.42	17	8.24	-0.338	Plasma membrane
VvXTH17	VIT_211s0052g01180	321	36,502.43	-	4.81	-0.596	Plasma membrane
VvXTH18	VIT_211s0052g01190	369	41,704.56	-	6.36	-0.454	Plasma membrane
VvXTH19	VIT_211s0052g01200	297	32,951.68	29	5.22	-0.392	Plasma membrane
VvXTH20	VIT_211s0052g01220	285	31,821.45	19	5.92	-0.404	Plasma membrane
VvXTH21	VIT_211s0052g01230	278	31,187.75	-	5.13	-0.405	Plasma membrane
VvXTH22	VIT_211s0052g01250	312	35,059.55	-	8.42	-0.338	Plasma membrane
VvXTH23	VIT_211s0052g01260	296	32,919.61	26	5.07	-0.393	Plasma membrane
VvXTH24	VIT_211s0052g01270	297	33,155.89	29	4.97	-0.361	Plasma membrane
VvXTH25	VIT_211s0052g01280	296	32,939.66	26	5.63	-0.420	Plasma membrane
VvXTH26	VIT_211s0052g01300	280	31,322.79	26	5.37	-0.419	Plasma membrane
VvXTH27	VIT_211s0052g01310	269	30,176.71	29	5.69	-0.275	Plasma membrane
VvXTH28	VIT_211s0052g01320	296	33,018.79	26	5.93	-0.425	Plasma membrane
VvXTH29	VIT_211s0052g01330	262	29,508.94	18	5.62	-0.459	Plasma membrane
VvXTH30	VIT_211s0052g01340	272	29,935.10	29	4.96	-0.457	Plasma membrane
VvXTH31	VIT_212s0134g00160	296	33,657.80	27	5.60	-0.320	Plasma membrane
VvXTH32	VIT_215s0048g02850	322	37,077.07	23	6.11	-0.346	Extracellular
VvXTH33	VIT_216s0100g00170	251	28,460.18	-	6.65	-0.232	Extracellular
VvXTH34	VIT_217s0053g00610	284	32,329.43	21	5.50	-0.361	Plasma membrane

Note:

AA, amino acid; MW, molecular weight; SP, signal peptide; pI, isoelectric point; GRAVY, total average hydrophilicity.

localization, revealed that they contained 251~369 AAs. The MW ranged from 28.5 to 41.7 kDa, while the pI ranged from 4.61 to 9.45. All XTHs exhibited hydrophilicity. Subcellular location prediction results showed that most of the genes are localized in the plasma membrane (29), while a few were localized extracellularly (5), including VvXTH10 and VvXTH12 in group IIIA and VvXTH2, VvXTH32, and VvXTH33. The majority of the proteins (80%) contained signal peptides, which were approximately 25-AA long (Table 1).

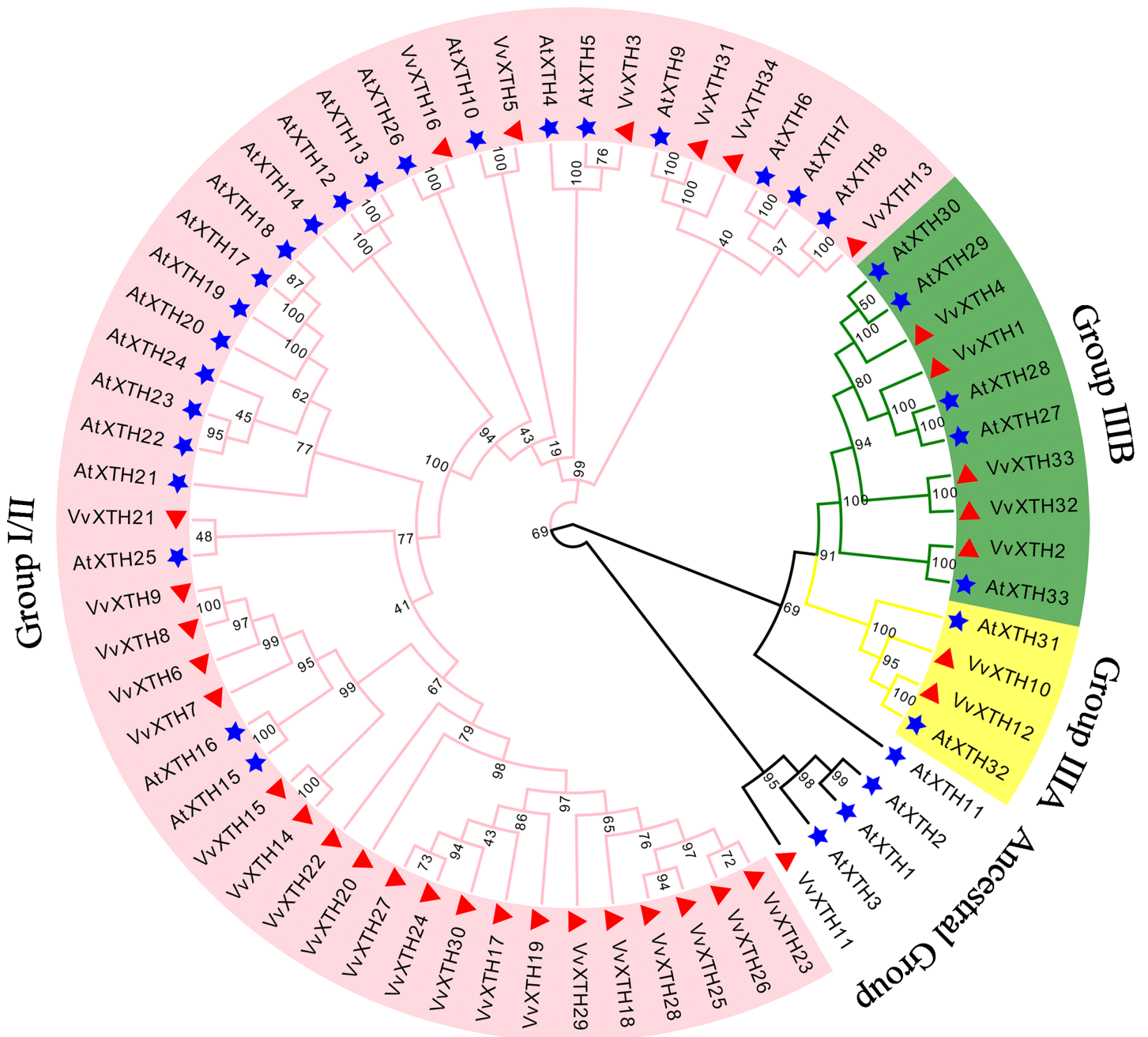


Figure 1 Phylogenetic analysis of XTHs of *Arabidopsis* and grapevine. The amino acid-based phylogenetic tree was generated using MEGA11.0 software *via* the neighbor-joining method. Bootstrap test results are indicated in the tree. The different colored branches and arcs represent Group I/II, IIIA, IIIB, and the Ancestral Group, and the blue five-pointed star represents *AtXTH* family members. The red triangle represents *VvXTH* family members. Full-size DOI: 10.7717/peerj.13546/fig-1

Phylogenetic analysis and classification of VvXTHs

To investigate the evolutionary relationships and functional associations of VvXTHs with AtXTHs, we built a phylogenetic tree utilizing the protein sequences of XTHs from *Vitis vinifera* and *Arabidopsis* (Fig. 1). The VvXTHs were grouped according to the previous grouping method applied for AtXTHs and the evolutionary relationship between grapes

and *Arabidopsis*. The results of the phylogenetic analysis indicated that the 34 *VvXTHs* could be divided into three groups, including 27 *VvXTHs* in group I/II, two in group IIIA, and five in group IIIB. In addition, one XTH protein (*VvXTH11*) was classified into the original ancestral group. Group I/II contained most of the members, and substantial similarity could be observed between some members of the group. The termini of the phylogenetic tree branch showed a total of 22 sister pairs, eight of which were orthologous pairs between *Arabidopsis* and grapevine, and six were grape homolog gene pairs. This analysis revealed that the number of *VvXTHs* was slightly expanded in comparison to the number of *XTHs* in *Arabidopsis*.

Thirty-four *VvXTHs* were unevenly distributed on 13 chromosomes. In particular, Chr.11 contained the largest number of *VvXTHs* (15), whereas other chromosomes contained considerably fewer genes. For example, a total of 4, 3, and 2 genes were located on Chr.5, Chr.10 and Chr.1, respectively. In addition, Chr.2, Chr.3, Chr.6, Chr.7, Chr.8, Chr.12, Chr.15, Chr.16, and Chr.17 each contained only one gene (Fig. 2A). Therefore, it can be inferred that there should be no observable association between the number of *XTHs* and the length of chromosomes. Furthermore, the genes located on Chr.11 and Chr.5 were closely clustered together. According to the chromosome location and genome annotation information, a total of 81 tandem duplicate gene pairs were obtained (Fig. 2A). To determine the relationships among *VvXTH* members, we performed a collinearity analysis and found no *VvXTH* within the identified collinear blocks, which indicated that segmental duplication is not involved in *VvXTH* expansion (Fig. 2B). These results prove that the expansion of *VvXTHs*, especially group I/II gene members, was driven by tandem duplication. We also traced the duplication time of *VvXTHs* by analyzing their K_a , K_s and K_a/K_s ratio. The K_a/K_s ratios of all *VvXTHs* were less than 1, ranging from 0.07 to 0.28. The duplication times of all *VvXTHs* were also calculated. The duplication times ranged from 2.91–78.39 Mya (million years ago) (Table S2). To further evaluate the evolution and development of the *VvXTH* family, we constructed a comparison diagram of grapes and *Arabidopsis*. Eight *VvXTHs* were shown to be synonymous with *XTHs* of *Arabidopsis*. Among these genes, *VvXTH10* is collinear with *AtXTH31* and *AtXTH32* in *Arabidopsis*, while *VvXTH1* is collinear with *AtXTH27* and *AtXTH28* in *Arabidopsis* (Fig. 2C). It is speculated that there may be functional redundancy among these genes, which implies that they have important roles in evolutionary progress.

Gene structural and multiple sequence alignment analysis of *VvXTHs*

Gene structural analysis revealed that the closely related genes within this subfamily are characterized by a similar structure, which can be further verified by the results of phylogenetic analysis (Fig. 3A). With the exception of *VvXTH32*, which lacks any introns, all other *VvXTH* members contain 2~4 different introns. In particular, group I/II contains a large number of members, and most members have two introns. The gene sister pairs, including *VvXTH23/26*, *VvXTH25/28*, *VvXTH14/15*, and *VvXTH8/9* at the terminal branch of the evolutionary tree, have highly similar exon/intron structures. In addition, compared with the adjacent gene *VvXTH27*, *VvXTH24* has lost an exon and exhibits

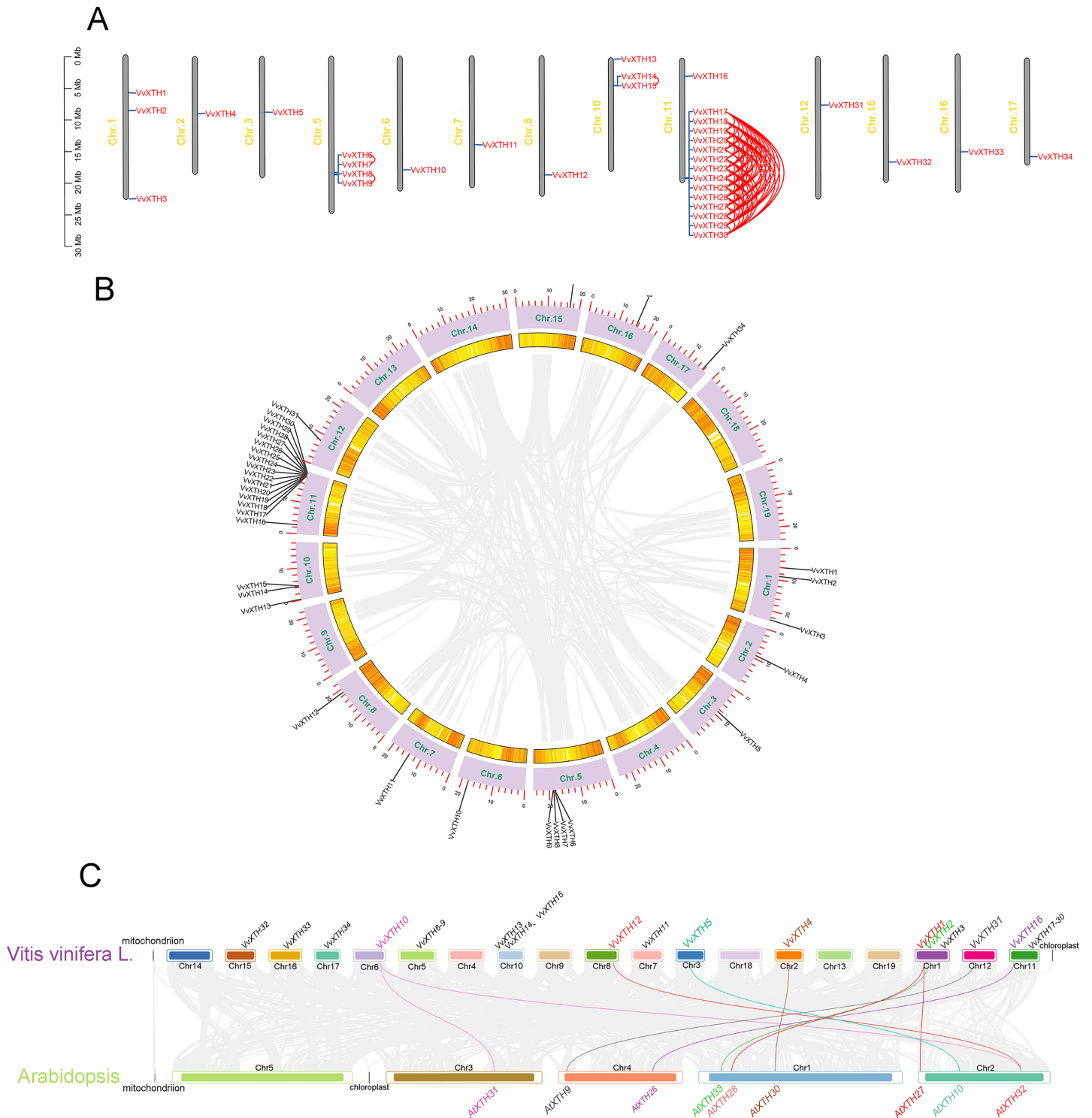


Figure 2 Systematic analysis of *VvXTHs* in grapevine. (A) Thirty-four *VvXTHs* were mapped on grape chromosomes based on their physical positions. Eighty-one tandemly duplicated gene pairs are indicated by red lines. The scale on the left is in megabases (Mb). (B) Schematic representations of the chromosomal distribution and interchromosomal relationships of *VvXTHs*. Gray lines indicate all syntenic blocks in the grape genome. Gene IDs on the chromosomes indicate gene physical positions. (C) Gray lines in the background indicate the collinear blocks identified in grape and *Arabidopsis*, while the different colored lines highlight the syntenic *XTH* gene pairs. [Full-size !\[\]\(b345a1c4255362eec3746050dd71ccac_img.jpg\) DOI: 10.7717/peerj.13546/fig-2](https://doi.org/10.7717/peerj.13546/fig-2)

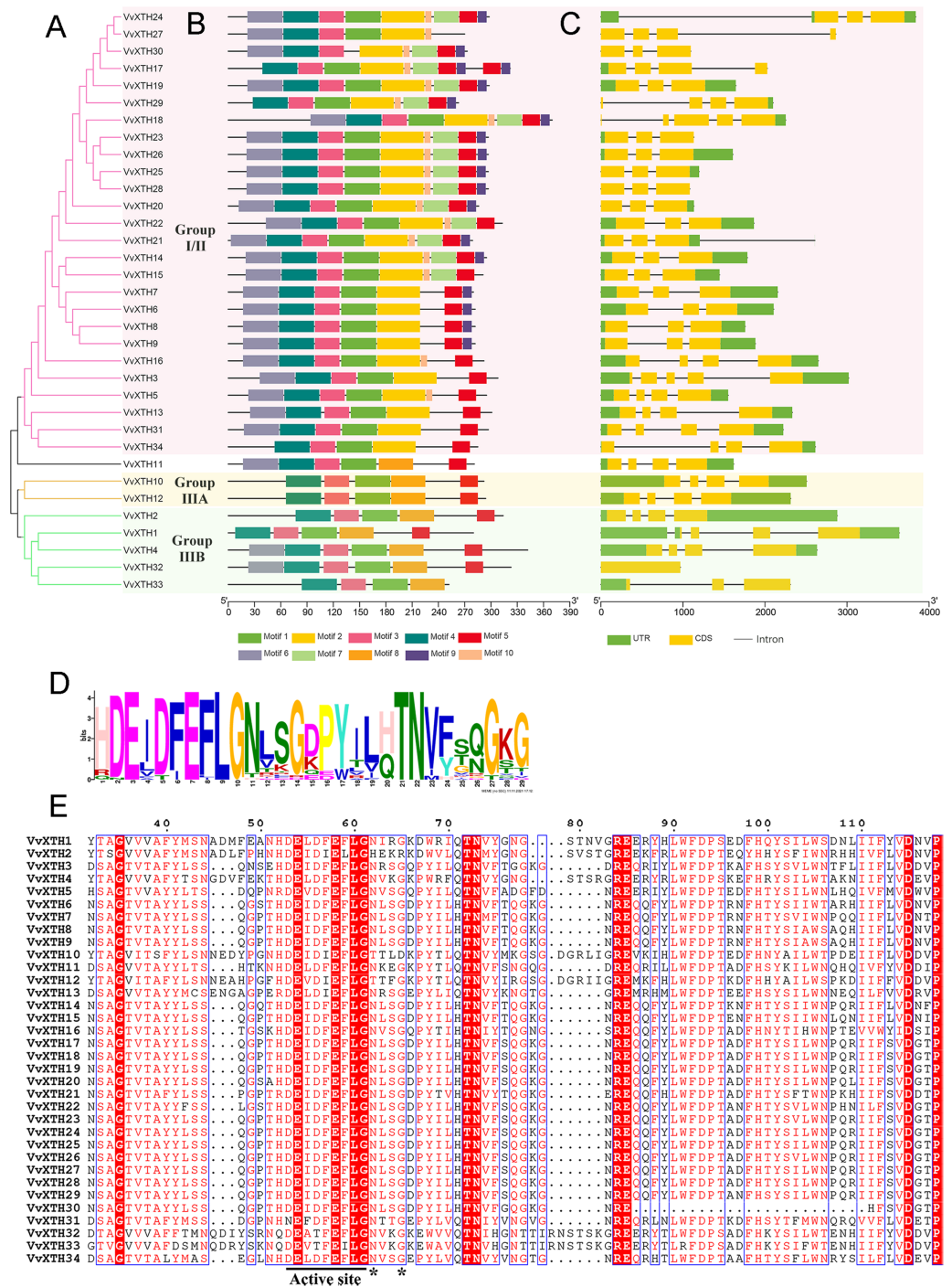


Figure 3 Phylogenetic relationships, structures and conserved motifs of VvXTHs. (A) Phylogenetic tree inferred from the protein sequences of VvXTHs. Branch colors represent different groups. (B) The motif composition of the VvXTHs identified using MEME. The different colored boxes represent different motifs and their positions in each VvXTH sequence. Each motif is indicated by a colored box in the legend at the bottom. (C) Gene structure of VvXTHs. The boxes represent exons or untranslated regions (UTRs), and lines represent introns. (D) Schematic representation of the conserved domains found in grape. (E) Multiple sequence alignments of the conserved domains of the VvXTHs. The black lines indicate the conserved domains. N-glycosylation residues are indicated with asterisks.

Full-size DOI: 10.7717/peerj.13546/fig-3

different intron and exon lengths. The members of group IIIA all have three introns and four exons and present high structural similarity. The members of group IIIB have developed different numbers and lengths of intron/exon structures during the long evolutionary process (Fig. 3C). In general, most *VvXTHs* present the same intron/exon structure pattern and remain conserved during evolution, which is consistent with the results obtained in other plants.

Based on the results of MEME motif analysis, motif three and motif four are highly conserved in all *VvXTHs*. Motif three is a characteristic domain that catalyzes enzymatic contact reactions, which denoted as (D/N)E(I/L/A/V/F)(D/T)(F/I)E(F/I/L)LG (Figs. 3B and 3D). Among these, the first glutamate residue (E) indicates the catalytic nucleophile that initiates the enzymatic reaction, and the second E residue functions represents a base to activate the entrant substrate. In addition, all members except for *VvXTH30* contain motif one; moreover, members of the same group share a similar motif composition (Fig. 3B). For instance, motif two only exists in group I/II, and motif eight only exists in group IIIA and IIIB. Genes in the same clade, especially those that are closely related, such as (1) *VvXTH23*, *VvXTH26*, *VvXTH25*, and *VvXTH28*; (2) *VvXTH6*, *VvXTH7*, *VvXTH8*, and *VvXTH9*; and (3) *VvXTH10* and *VvXTH12*, can share much more similar motif structures (Fig. 3B). In addition, motif seven, motif nine, and motif 10 only exist in group I/II, and most of the group members contain the motifs mentioned above (Fig. 3B). The members of group IIIA contain five motifs with the same distribution. Group IIIB members contain 4–6 motifs; while they all share four identical motifs, only *VvXTH4* and *VvXTH32* have motif six, and only *VvXTH33* does not have motif five. The results of multiple sequence alignment also confirmed that the conserved domain active site is present in all *VvXTHs*. Moreover, with the exception of *VvXTH2* (IIIB), *VvXTH10* (IIIA), and *VvXTH12* (IIIA), potential N-glycosylation residues are located near the active site in the 31 other *VvXTHs* (Fig. 3E). Conserved domain predictions suggested that members of the same subfamily may have similar structures and may be involved in similar functions. Thus, we need to focus on distinctive members that may present surprising functions that remain to be discovered.

Organ-specific expression pattern analysis of *VvXTHs*

Through the expression profile (GSE36128) analysis of the GEO data set, we obtained the specific expression patterns of *VvXTH* members in different organs and developmental periods of grapevine to predict the functions of *VvXTHs* in growth and development (Fig. 4). According to the results of cluster analysis, the *VvXTH* families were classified into four groups (A–D): group A contains seven genes with high expression levels in berry peels, skins, shafts, and tendrils; group B includes four members with high expression levels only in stems and tendrils but low expression in other organs; group C includes eight genes with very low expression levels in all organs; and group D is the largest (15 members) subfamily and shows the highest expression in berries, shafts, and tendrils. In addition, the *VvXTHs* had higher expression levels in the pulp, peel, and stem during the V (veraison), MR (mid-ripening), and R (ripening) periods, indicating that *VvXTHs* may be related to fruit ripening. In short, the four groups of *VvXTHs* present specific expression

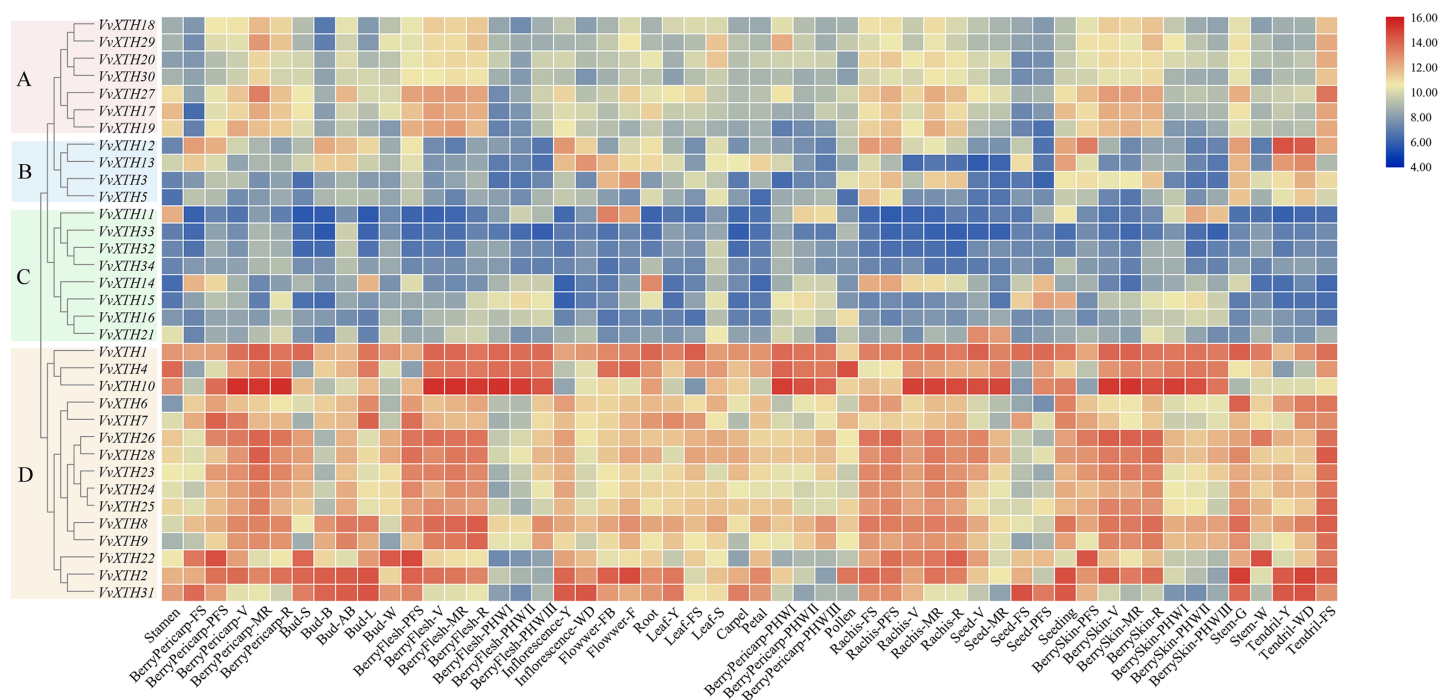


Figure 4 Expression patterns of *VvXTHs* in different organs and developmental stages. Rows represent *VvXTH* members, while columns represent different developmental stages and organs. The expression levels of *VvXTHs* are indicated by the intensity of color. The phylogenetic tree on the left side of the heatmap is based on the hierarchical clustering of the expression profiles of *VvXTHs* in 54 samples.

Full-size [DOI: 10.7717/peerj.13546/fig-4](https://doi.org/10.7717/peerj.13546/fig-4)

profiles depending on the organ and developmental stage. This interesting phenomenon may be due to the specific functions of these specific genes in related tissues.

To verify the reliability of the organ-specific expression profiles, qRT-PCR analysis was conducted on five different tissues (tendril, root, stem, leaf and flower) of grapevine “Crimson” for *VvXTHs*, then the qRT-PCR results were compared with the data obtained from the GSE36128 data set of the cultivar “Corvina” (Marianna et al., 2012) with the same tissues at the corresponding developmental stages. It was found that the expression patterns of *VvXTHs* were generally consistent with the data obtained from the GSE36128 data set (Fig. S2), which suggests that temporal and spatial expression of *VvXTHs* is generally similar in different cultivars, even grown in different conditions.

Transcriptional profiles of *VvXTHs* under abiotic stress

The PlantCARE database and New PLACE database were utilized to identify *cis*-elements in the DNA sequences 1.5 KB upstream of the *VvXTH* start codons. The results showed that all 34 *VvXTHs* contained a variety of abiotic and biotic stress response elements, phytohormone response elements, and growth and development-related response elements (Fig. 5A). Similarly, in the New PLACE database, all 34 *VvXTHs* were predicted to contain phytohormone response elements and elements involved in the responses to a variety of abiotic stresses, including cold and heat, ABA, dehydration and salinity (osmotic) stress (Fig. 5B). As shown in Fig. S3, two drought stress response elements

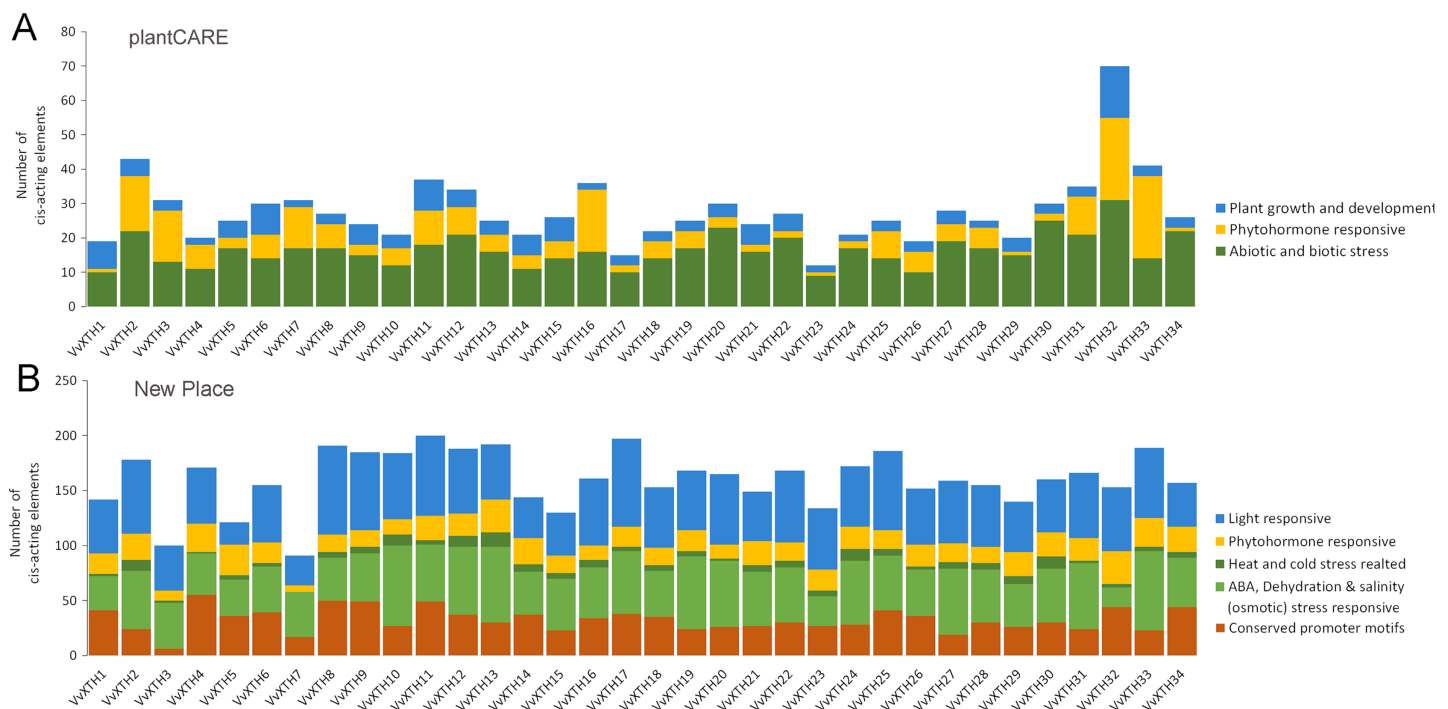


Figure 5 Cis-element analysis in the promoter regions 1,500 bp upstream of the start codons of *VvXTHs*. The prediction analysis was performed by using plantCARE (A) and New PLACE (B). The bar graphs represent the total number of *cis*-elements in each gene promoter region. Different colors represent different types of *cis*-elements. Three types of *cis*-elements were predicted in plantCARE. Five types of *cis*-elements were predicted in New PLACE.

Full-size DOI: 10.7717/peerj.13546/fig-5

(MYB and MYC) exist in almost all members, and 80% of the gene members contain defense and stress response elements (STREs), which indicates that the *VvXTH* family probably shows important functions when plants are subjected to abiotic or biotic stress. Abscisic acid response elements (ABREs) and salicylic acid response elements (TCA elements) are abundantly present in *VvXTH* family members, which indicates that the *VvXTH* family may also be involved in hormone regulation during plant growth and the response to stress. The presence of a meristem development control element (CAT-box) in most *VvXTH* members suggests that the *VvXTH* family may have significant effects on the regulation of plant growth and development. In particular, the 34 *VvXTHs* were predicted to contain a large number of light response elements in the New PLACE database, and light-responsive elements (GATABOX and Box-4) were present in most *VvXTH* members, suggesting that the *VvXTH* family plays important roles in photosynthesis and photomorphogenesis.

Promoter analysis demonstrated the widespread presence of *cis*-elements associated with abiotic stress in the promoter regions of *VvXTHs*, revealing the possible induction of *VvXTH* expression by abiotic stress. To further investigate the potential roles of *VvXTHs* in response to abiotic stress, especially drought stress and salt stress, we selected 14 *VvXTH* members harboring abiotic response *cis*-elements for further study. Six-week-old grape seedlings were exposed to 200 mM NaCl or 200 mM mannitol, and the expression of 14 *VvXTHs* was examined in separated leaves and roots. In roots, the

expression levels of 11 genes were upregulated under salt stress, among which four members were significantly upregulated. The expression of *VvXTH5*, *VvXTH20*, and *VvXTH34* was increased by more than two-fold, and that of *VvXTH4* was increased by more than four-fold. Interestingly, the expression of *VvXTH4* peaked after 9 h of treatment, presenting an obviously different pattern from the other genes. This shows that these genes may respond to salt stress in different ways. Under drought stress, most of the genes whose expression was upregulated reached a peak after 3 h of treatment, and some genes were upregulated by more than four-fold (*VvXTH3* and *VvXTH20*). *VvXTH10* expression reached a peak after 12 h of treatment, indicating that this gene may be expressed at a later time. The number of upregulated *VvXTHs* in leaves relative to roots decreased after stress treatment, but these genes were more highly upregulated. Among these genes, *VvXTH3*, *VvXTH10*, and *VvXTH31* were upregulated by approximately ten-fold. The above genes might play particularly crucial roles in the leaf response to salinity stress. Taken together, our findings indicate that the expression of *VvXTHs* could be altered by salt and drought stress, suggesting that *VvXTHs* may participate in reactions to abiotic damage, especially under salt and drought stress.

DISCUSSION

The *XTH* family consists of modification enzymes that can rebuild cell walls by modulating the construction and composition of xyloglucan cross-links (Campbell & Braam, 2010). According to previous studies, various members of this family have been identified in *Arabidopsis thaliana*, *Oryza sativa*, *Medicago truncatula*, *Nicotiana tabacum*, *Solanum lycopersicum*, and *Ananas comosus*, and these proteins have been verified to play critical roles in development, biotic stress, and abiotic stress (Meng et al., 2018; Li et al., 2019b; Yokoyama, 2004; Kurasawa et al., 2009; Xuan et al., 2016). The release of the most recent grape genome database made it possible to identify the grape *XTH* family (Ariga, Muneyuki & Yoshida, 2007). In this study, thirty-four *VvXTHs* were systematically identified and characterized using bioinformatics approaches. The results showed that the number of identified *VvXTHs* (34) (Fig. 1) was slightly greater than the numbers found in *Arabidopsis thaliana* (33) and *Oryza sativa* (29) (Yokoyama, 2004; Kurasawa et al., 2009), which may be related to pedigree-specific gains and losses as well as gene duplication events. Gene duplication is a primary driver of the expansion of gene families, and tandem duplications and segmental duplications are considered the primary duplication modes (Zhu et al., 2014). Previous studies of the *XTH* family have also reported gene tandem duplications or segmental duplications in barley, soybean, and tobacco (Fu, Liu & Wu, 2019; Li et al., 2018; Meng et al., 2018).

Interestingly, we observed that the thirty-four identified *VvXTHs* were located on 13 chromosomes, and Chr.11 and Chr.5 contained gene clusters (Fig. 2). Based on the definition of gene tandem duplication, *VvXTH17-VvXTH30* and *VvXTH6-VvXTH9* represent gene tandem duplication events. According to the analysis of the Ka/Ks ratio (Table S2), all genes showed ratios of less than 1, which indicates that they are under intense purifying selection (Hurst, 2002). Hence, the role of gene tandem duplication in

VvXTH family expansion, particularly in increasing the number of VvXTH members and their functional diversification, is irreplaceable.

According to gene function and Clustal analyses, similar to other plants, the 34 VvXTHs are divided into groups I/II, IIIA, and IIIB and an ancestral group (Fig. 1). According to previous studies, due to the unclear distinction between groups I and II, these subgroups were combined into one group (group I/II) (Campbell & Braam, 1999). The XTHs in group IIIA mainly display XEH activity, while those of group IIIB showed obvious XET activity, suggesting a functional distinction between groups IIIA and IIIB (Eklof & Brumer, 2010; Nomchit et al., 2010; Opazo et al., 2017). Serines or threonines located near the catalytic center of XET are typical residues for N-glycosylation, and the results of multiple sequence alignment showed that the members of groups I/II and IIIB (except for VvXTH2) contain N-glycosylated residues, while those of group IIIA do not (Mark et al., 2009). Therefore, we speculated that VvXTH10 and VvXTH12 proteins in group IIIA might possess XEH activity and that VvXTH4, VvXTH32 and VvXTH33 proteins in group IIIB might show XET activity in grape, which is in agreement with previous research findings (Fig. 1) (Mark et al., 2009; Miedes & Lorences, 2009).

The analysis of gene structure is of great significance to further clarify the origins, evolution, and genetic relationships of species. XTH family members show a relatively wide variety of structures. Specifically, most members of the grape XTH family contain three or four introns (Fig. 2C), while others have fewer intron, which may be related to gene splicing (Mount et al., 2012). It is precisely because of the existence of multiple introns that gene splicing becomes more complicated, and the number of different XTH expression products increases. According to a comparison of the AA sequences of *Arabidopsis thaliana*, *Populus tomentosa*, *Hordeum vulgare*, *Brassica rapa*, and *Brassica oleracea*, even when the difference in protein size is obvious, the active-site domain is still conserved in the reported XTH proteins (An et al., 2017). In this study, all 34 VvXTHs were found to contain motif three (Opazo et al., 2017), which suggests that XTH proteins may play similar roles in the plant kingdom. It has been reported that the active site mediates catalytic activity, which can catalyze hydrolase activity and carry out cell wall structural modification and rearrangement by cutting and repolymerizing cellulose single chains (Li et al., 2018; Behar, Graham & Brumer, 2018). The cross-linked xyloglucan structure has critical functions in maturation and resistance to abiotic stress (Bulone, Schwerdt & Fincher, 2019).

Previous studies have shown that XTHs are of vital importance in plant resistance to abiotic stress (Chen et al., 2019; Dong et al., 2019; Li et al., 2019b). The expression of *CaXTH3* is induced by a variety of abiotic stresses, such as drought, high salt, and low temperature, and the tolerance of *CaXTH3* transgenic tomato plants to salt and drought stress is thereby significantly improved (Choi et al., 2011). Additionally, the heterologous expression of *PeXTH* in tobacco improves plant osmotic tolerance by reducing water loss and reducing the speed of stomatal opening (Han et al., 2014). To study the potential function of VvXTHs against abiotic stress, we carried out promoter analysis and tissue expression analysis (Figs. 3 and 4). The results indicated that the upstream promoter regions of almost all members of the grape XTH family contain MBS, MYB, MYC, and

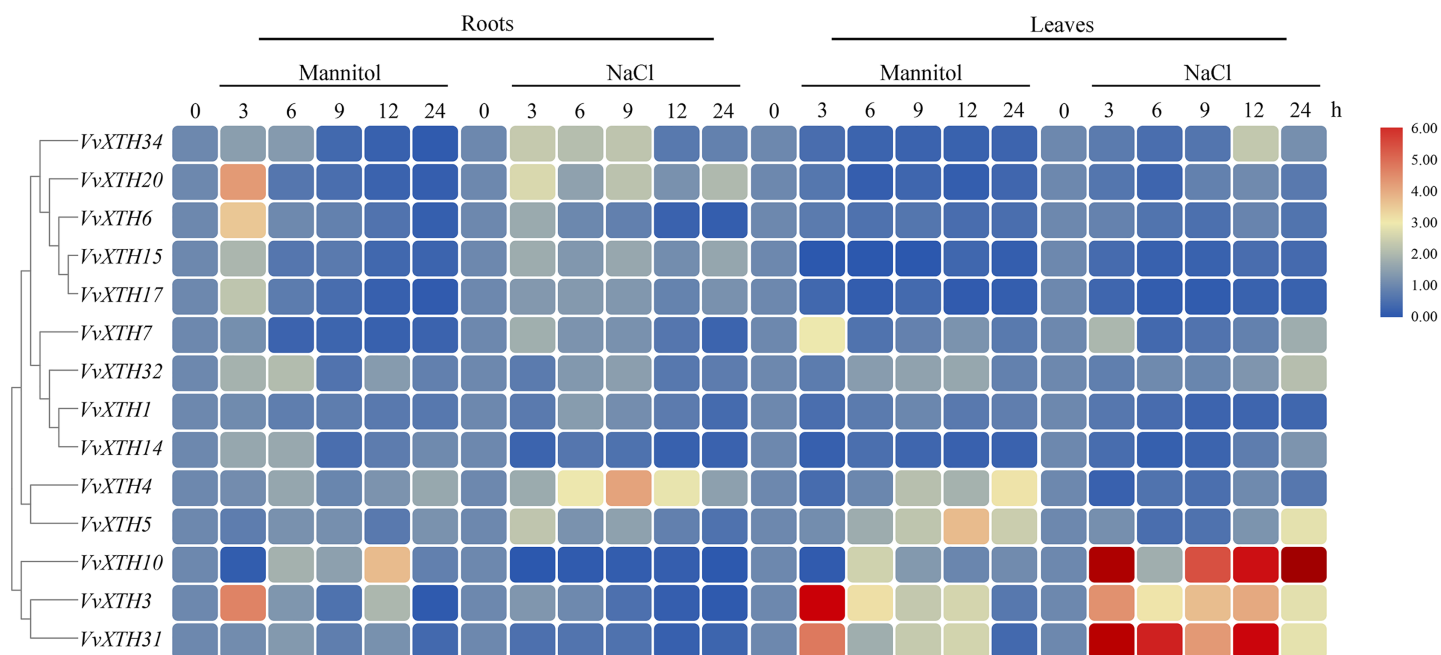


Figure 6 Expression profiles of *VvXTHs* under abiotic stress. Heatmap showing the relative expression of 14 *VvXTHs*, detected by qRT-PCR, in roots and leaves of 6-week-old "Crimson" grape seedlings after treatment with 200 mM NaCl and 200 mM mannitol for 0, 3, 6, 9, 12, and 24 h (0 h treatment as the control). Experiments were performed in biological triplicates. [Full-size !\[\]\(1663bb69f307a960345edb0e712f8c02_img.jpg\) DOI: 10.7717/peerj.13546/fig-6](https://doi.org/10.7717/peerj.13546/fig-6)

ARE *cis*-elements for responding to drought stress. Furthermore, 47% of these sequences contain ABREs, to respond to ABA (Fig. 4). Under drought conditions, ABA inhibits root growth and development, represses seed germination, and promotes the shedding of senescent tissues and organs (Hirayama & Shinozaki, 2007). Some *VvXTHs* exist in the mature stage, and ABA may promote *XTH* expression and affect organ abscission (Figs. 3 and 6). In addition, a few members of the *VvXTH* family also contain DRE action elements, which means that *XTHs* can potentially respond to salt stress, in addition to drought stress (Fig. 5). It is also interesting that the expression of *VvXTHs* varies in different organs. Genes from the same gene cluster of gene tandem repeat events, such as *VvXTH6* and *VvXTH7* or *VvXTH26*, and *VvXTH30*, show differences in expression in organs at different stages. These results implied that during evolution, closely related genes have undergone subfunctional evolution, functionalization or nonfunctionalization, helping grapes adapt to a variety of growth environments. The expression profiling of *VvXTHs* under different stresses revealed the induction of *VvXTH3*, *VvXTH31*, and *VvXTH10* in roots.

Taken together, these findings provide novel information about *VvXTHs* under abiotic stress, especially drought and salt stresses. It can be speculated that the above genes may show increased cell wall-related functions under stress by combining with xyloglucan. Nevertheless, further molecular and genetic identification efforts are needed to verify their functions.

CONCLUSIONS

In this study, 34 *XTHs*, which could be further divided into group I/II, group IIIA, and group IIIB, were successfully isolated and identified in grapevine. It was shown that the *VvXTHs* are unevenly distributed on 13 chromosomes. According to collinearity analysis, tandem duplication of genes may have occurred on Chr.5 and Chr.11. Furthermore, all *VvXTHs* contain conserved XTH domains and active sites. Expression analysis showed that some *VvXTHs* can effectively respond to salt and drought stress at the transcriptional level. In this context, the results of the present investigation will lay a foundation for future investigations of the function of *VvXTHs*.

ADDITIONAL INFORMATION AND DECLARATIONS

Funding

The present study was supported by the National Natural Science Foundation of China (31972358), the Natural Science Foundation of Shandong Province, China (ZR2018MC022), and the Shandong Provincial Key Research and Development Project (2019JZZY010727 and 2019GNC106147). The funders had no role in study design, data collection and analysis, decision to publish, or preparation of the manuscript.

Grant Disclosures

The following grant information was disclosed by the authors:

National Natural Science Foundation of China: 31972358.

Natural Science Foundation of Shandong Province, China: ZR2018MC022.

Shandong Provincial Key Research and Development Project: 2019JZZY010727 and 2019GNC106147.

Competing Interests

The authors declare that they have no competing interests.

Author Contributions

- Tian Qiao conceived and designed the experiments, performed the experiments, analyzed the data, prepared figures and/or tables, authored or reviewed drafts of the article, and approved the final draft.
- Lei Zhang conceived and designed the experiments, performed the experiments, analyzed the data, prepared figures and/or tables, authored or reviewed drafts of the article, and approved the final draft.
- Yanyan Yu performed the experiments, prepared figures and/or tables, and approved the final draft.
- Yunning Pang performed the experiments, prepared figures and/or tables, and approved the final draft.
- Xinjie Tang analyzed the data, prepared figures and/or tables, and approved the final draft.

- Xiao Wang analyzed the data, prepared figures and/or tables, and approved the final draft.
- Lijian Li analyzed the data, prepared figures and/or tables, and approved the final draft.
- Bo Li conceived and designed the experiments, authored or reviewed drafts of the article, and approved the final draft.
- Qinghua Sun conceived and designed the experiments, authored or reviewed drafts of the article, and approved the final draft.

Data Availability

The following information was supplied regarding data availability:

The raw data are available in the [Supplemental File](#).

Supplemental Information

Supplemental information for this article can be found online at <http://dx.doi.org/10.7717/peerj.13546#supplemental-information>.

REFERENCES

- An Y, Yang J, Liu Z, Zhang G, Ma Z, Wang X. 2017. Genome-wide identification and expression analysis of the *XTH* gene family in fiber development process in *Gossypium hirsutum* L. *Journal of Plant Genetic Resources* **18**:1179–1192 DOI [10.13430/j.cnki.jpgr.2017.06.020](https://doi.org/10.13430/j.cnki.jpgr.2017.06.020).
- Araujo JA, Abiodun BJ, Crespo O. 2016. Impacts of drought on grape yields in Western Cape, South Africa. *Theoretical Applied Climatology* **123**:117–130 DOI [10.1007/s00704-014-1336-3](https://doi.org/10.1007/s00704-014-1336-3).
- Ariga T, Muneyuki E, Yoshida M. 2007. F1-ATPase rotates by an asymmetric, sequential mechanism using all three catalytic subunits. *Nature Structural & Molecular Biology* **14**(17):841–846 DOI [10.1038/nsmb1296](https://doi.org/10.1038/nsmb1296).
- Bailey TL, Mikael B, Buske FA, Martin F, Grant CE, Luca C, Jing R, Li WW, Noble WS. 2009. MEME Suite: tools for motif discovery and searching. *Nucleic Acids Research* **37**(Web Server):W202–W208 DOI [10.1093/nar/gkp335](https://doi.org/10.1093/nar/gkp335).
- Balakrishnan S, Gao S, Lercher MJ, Hu S, Chen W. 2019. Evolview v3: a webserver for visualization, annotation, and management of phylogenetic trees. *Nucleic Acids Research* **47**(W1):W270–W275 DOI [10.1093/nar/gkz357](https://doi.org/10.1093/nar/gkz357).
- Baumann MJ, Eklof JM, Michel G, Kallas AM, Teeri T, Czjzek M, Brumer H. 2007. Structural evidence for the evolution of xyloglucanase activity from xyloglucan endo-transglycosylases: biological implications for cell wall metabolism. *Plant Cell* **19**(6):1947–1963 DOI [10.1105/tpc.107.051391](https://doi.org/10.1105/tpc.107.051391).
- Behar H, Graham SW, Brumer H. 2018. Comprehensive cross-genome survey and phylogeny of glycoside hydrolase family 16 members reveals the evolutionary origin of EG16 and XTH proteins in plant lineages. *Plant Journal* **95**(6):1114–1128 DOI [10.1111/tpj.14004](https://doi.org/10.1111/tpj.14004).
- Bulone V, Schwerdt JG, Fincher GB. 2019. Co-evolution of enzymes involved in plant cell wall metabolism in the grasses. *Front Plant Science* **10**:1009 DOI [10.3389/fpls.2019.01009](https://doi.org/10.3389/fpls.2019.01009).
- Campbell P, Braam J. 1999. Xyloglucan endotransglycosylases: diversity of genes, enzymes and potential wall-modifying functions. *Trends in Plant Science* **4**(9):361–366 DOI [10.1016/S1360-1385\(99\)01468-5](https://doi.org/10.1016/S1360-1385(99)01468-5).
- Campbell P, Braam J. 2010. Co- and/or post-translational modifications are critical for TCH4 XET activity. *Plant Journal* **15**(4):553–561 DOI [10.1046/j.1365-313X.1998.00239.x](https://doi.org/10.1046/j.1365-313X.1998.00239.x).

- Canaguier A, Grimplet J, Gaspero GD, Scalabrin S, Duchêne E, Choisine N, Mohellibi N, Guichard C, Rombauts S, Clainche IL. 2017. A new version of the grapevine reference genome assembly (12X.v2) and of its annotation (VCost.v3). *Genomics Data* **14**(3):56–62 DOI [10.1016/j.gdata.2017.09.002](https://doi.org/10.1016/j.gdata.2017.09.002).
- Cao H, Liu CY, Liu CX, Zhao YL, Xu RR. 2016. Genomewide analysis of the lateral organ boundaries domain gene family in *Vitis vinifera*. *Journal of Genetics* **95**(3):515–526 DOI [10.1007/s12041-016-0660-z](https://doi.org/10.1007/s12041-016-0660-z).
- De Caroli M, Manno E, Piro G, Lenucci MS. 2021. Ride to cell wall: *Arabidopsis XTH11*, *XTH29* and *XTH33* exhibit different secretion pathways and responses to heat and drought stress. *The Plant Journal* **107**(2):448–466 DOI [10.1111/tpj.15301](https://doi.org/10.1111/tpj.15301).
- Chen D, Qi Q, Wang Z, Sun X, Yang F, Guo XM, Song XY. 2019. Cloning and expression of *ZmXTH23* in maize (*Zea mays*) and its response to salt and drought stress. *Journal of Agricultural Biotechnology* **27**:1533–1541 DOI [10.3969/j.issn.1674-7968.2019.09.002](https://doi.org/10.3969/j.issn.1674-7968.2019.09.002).
- Cheng Z, Zhang X, Yao W, Gao Y, Zhao K, Guo Q, Zhou B, Jiang T. 2021. Genome-wide identification and expression analysis of the xyloglucan endotransglucosylase/hydrolase gene family in poplar. *BMC Genomics* **22**(1):804 DOI [10.1186/s12864-021-08134-8](https://doi.org/10.1186/s12864-021-08134-8).
- Choi J, Seo YS, Kim WT, Shin JS. 2011. Constitutive expression of *CaXTH3*, a hot pepper xyloglucan endotransglucosylase/hydrolase, enhanced tolerance to salt and drought stresses without phenotypic defects in tomato plants (*Solanum lycopersicum* cv *Dotaerang*). *Plant Cell Reports* **30**(5):867–877 DOI [10.1007/s00299-010-0989-3](https://doi.org/10.1007/s00299-010-0989-3).
- Daisuke T, Peng H, Tan T, Alexander E, Arun S, Antony B, Joachim K, Takeshi K, Ryusuke Y, Kazuhiko N, Ellen Z. 2020. Cell wall modification by the xyloglucan endotransglucosylase/hydrolase *XTH19* influences freezing tolerance after cold and sub-zero acclimation. *Plant, Cell & Environment* **44**(3):915–930 DOI [10.1111/pce.13953](https://doi.org/10.1111/pce.13953).
- Dan MB, Staines DM, Perry E, Kersey PJ. 2017. Ensembl plants: integrating tools for visualizing, mining, and analyzing plant genomics data. *Methods in Molecular Biology* **1533**:1–13 DOI [10.1007/978-1-4939-6658-5_1](https://doi.org/10.1007/978-1-4939-6658-5_1).
- Dong C, Wei Y, Wang Y, Zheng X, Li W. 2019. Identification and analysis of xyloglucan endotransglucosylase/hydrolase (*XTH*) family gene in *Litchi chinensis* based on transcriptome. *Molecular Plant Breeding* **17**:3865–3873 DOI [10.13271/j.mpb.017.003865](https://doi.org/10.13271/j.mpb.017.003865).
- Duvaud S, Gabella C, Lisacek F, Stockinger H, Durinx C. 2021. Expasy, the Swiss Bioinformatics Resource Portal, as designed by its users. *Nucleic Acids Research* **49**(W1):W216–W227 DOI [10.1093/nar/gkab225](https://doi.org/10.1093/nar/gkab225).
- Eklöf JM, Brumer H. 2010. The *XTH* gene family: an update on enzyme structure, function, and phylogeny in xyloglucan remodeling. *Plant Physiology* **153**(2):456–466 DOI [10.1104/pp.110.156844](https://doi.org/10.1104/pp.110.156844).
- Feng R, He W, Hiroto O. 2000. Experimental studies on antioxidation of extracts from several plants used as both medicines and foods in vitro. *Journal of Chinese Medicinal Materials* **23**:690 DOI [10.1016/S0168-1702\(00\)00198-2](https://doi.org/10.1016/S0168-1702(00)00198-2).
- Fu MM, Liu C, Wu F. 2019. Genome-wide identification, characterization and expression analysis of xyloglucan endotransglucosylase/hydrolase genes family in barley (*Hordeum vulgare*). *Molecules* **24**(10):1935 DOI [10.3390/molecules24101935](https://doi.org/10.3390/molecules24101935).
- Gaia C, Alex B, Cath B, Petrov AI, Rahumans MS, Michele IS, Henning H, Paul F, Rolf A, Ewan B. 2021. The European Bioinformatics Institute (EMBL-EBI) in 2021. *Nucleic Acids Research* **50**(D1):D11–D19 DOI [10.1093/nar/gkab1127](https://doi.org/10.1093/nar/gkab1127).
- Han Y, Ban Q, Hou Y, Meng K, Suo J, Rao J. 2016. Isolation and characterization of two persimmon xyloglucan endotransglycosylase/hydrolase (*XTH*) genes that have divergent

- functions in cell wall modification and fruit postharvest softening. *Frontiers in Plant Science* 7:624 DOI 10.3389/fpls.2016.00624.
- Han S, Ban Q, Jin YH, Rao J. 2017. Overexpression of persimmon *DkXTH1* enhanced tolerance to abiotic stress and delayed fruit softening in transgenic plants. *Plant Cell Reports* 36(4):583–596 DOI 10.1007/s00299-017-2105-4.
- Han Y, Sa G, Sun J, Shen Z, Zhao R, Ding M, Deng S, Lu Y, Zhang Y, Shen X, Chen S. 2014. Overexpression of *Populus euphratica* xyloglucan endotransglucosylase/hydrolase gene confers enhanced cadmium tolerance by the restriction of root cadmium uptake in transgenic tobacco. *Environmental and Experimental Botany* 100:74–83 DOI 10.1016/j.envexpbot.2013.12.021.
- Han Y, Wang W, Sun J, Ding M, Zhao R, Deng S, Wang F, Hu Y, Wang Y, Lu Y, Du L, Hu Z, Diekmann H, Shen X, Polle A, Chen S. 2013. *Populus euphratica* XTH overexpression enhances salinity tolerance by the development of leaf succulence in transgenic tobacco plants. *Journal of Experimental Botany* 64(14):4225–4238 DOI 10.1093/jxb/ert229.
- Hirayama T, Shinozaki K. 2007. Perception and transduction of abscisic acid signals: keys to the function of the versatile plant hormone ABA. *Trends in Plant Science* 12(8):343–351 DOI 10.1016/j.tplants.2007.06.013.
- Hu B, Jin J, Guo AY, Zhang H, Luo J, Gao G. 2015. GSDS 2.0: an upgraded gene feature visualization server. *Bioinformatics* 31(8):1296–1297 DOI 10.1093/bioinformatics/btu817.
- Hurst LD. 2002. The Ka/Ks ratio: diagnosing the form of sequence evolution. *Trends in Genetics* 18(9):486–487 DOI 10.1016/S0168-9525(02)02722-1.
- Kurasawa K, Matsui A, Yokoyama R, Kuriyama T, Yoshizumi T, Matsui M, Suwabe K, Watanabe M, Nishitani K. 2009. The *AtXTH28* gene, a xyloglucan endotransglucosylase/hydrolase, is involved in automatic self-pollination in *Arabidopsis thaliana*. *Plant Cell Physiology* 50(2):413–422 DOI 10.1093/pcp/pcp003.
- Larkin MA, Blackshields G, Brown NP, Chenna R, McGettigan PA, McWilliam H, Valentin F, Wallace IM, Wilm A, Lopez R, Thompson JD, Gibson TJ, Higgins DG. 2007. Clustal W and Clustal X version 2.0. *Bioinformatics* 23(21):2947–2948 DOI 10.1093/bioinformatics/btm404.
- Li S, Babu V, Silvas P, Wan J, Henry N. 2018. Characterization of the XTH gene family: new insight to the roles in soybean flooding tolerance. *International Journal of Molecular Sciences* 19(9):2705 DOI 10.3390/ijms19092705.
- Li R, Ge H, Dai Y, Yuan L, Liu X, Sun Q, Wang X. 2019a. Genomewide analysis of homeobox gene family in apple (*Malus domestica* Borkh.) and their response to abiotic stress. *Journal of Genetics* 98(1):13 DOI 10.1007/s12041-018-1049-y.
- Li Q, Li H, Yin C, Wang X, Jiang Q, Zhang R, Ge F, Chen Y, Yang L. 2019b. Genome-wide identification and characterization of xyloglucan endotransglycosylase/hydrolase in *Ananas comosus* during development. *Genes* 10(7):537 DOI 10.3390/genes10070537.
- Liu GT, Jiang JF, Liu XN, Jiang JZ, Wang LJ. 2019. New insights into the heat responses of grape leaves via combined phosphoproteomic and acetylproteomic analyses. *Horticulture Research* 6(1):100 DOI 10.1038/s41438-019-0183-x.
- Liu YB, Lu SM, Zhang JF, Liu S, Lu YT. 2007. A xyloglucan endotransglucosylase/hydrolase involves in growth of primary root and alters the deposition of cellulose in *Arabidopsis*. *Planta* 226(6):1547–1560 DOI 10.1007/s00425-007-0591-2.
- Magali L, Patrice D, Gert T, Kathleen M, Yves M, Pierre R, Rombauts S. 2002. PlantCARE, a database of plant cis-acting regulatory elements and a portal to tools for in silico analysis of promoter sequences. *Nucleic Acids Research* 30(1):325–327 DOI 10.1093/nar/30.1.325.

- Marianna F, Silvia D, Sara Z, Giovanni B, Lorenzo F, Anita Z, Andrea P, Pezzotti M. 2012. The grapevine expression atlas reveals a deep transcriptome shift driving the entire plant into a maturation program. *Plant Cell* **24**(9):3489–3505 DOI [10.1105/tpc.112.100230](https://doi.org/10.1105/tpc.112.100230).
- Mark P, Baumann MJ, Eklof JM, Gullfot F, Michel G, Kallas AM, Teeri T, Brumer H, Czjzek M. 2009. Analysis of nasturtium *TmNXG1* complexes by crystallography and molecular dynamics provides detailed insight into substrate recognition by family GH16 xyloglucan endo-transglycosylases and endo-hydrolases. *Proteins-structure Function and Bioinformatics* **75**(4):820–836 DOI [10.1002/prot.22291](https://doi.org/10.1002/prot.22291).
- Matsui A, Yokoyama R, Seki M, Ito T, Shinozaki K, Takahashi T, Komeda Y, Nishitani K. 2005. *AtXTH27* plays an essential role in cell wall modification during the development of tracheary elements. *Plant Journal* **42**(4):525–534 DOI [10.1111/j.1365-3113X.2005.02395.x](https://doi.org/10.1111/j.1365-3113X.2005.02395.x).
- Meng W, Xu ZC, Anming D, Kong YZ. 2018. Genome-wide identification and expression profiling analysis of the xyloglucan endotransglucosylase/hydrolase gene family in tobacco (*Nicotiana tabacum* L.). *Genes* **9**(6):273 DOI [10.3390/genes9060273](https://doi.org/10.3390/genes9060273).
- Miedes E, Lorences EP. 2009. Xyloglucan endotransglucosylase/hydrolases (XTHs) during tomato fruit growth and ripening. *Journal of Plant Physiology* **166**(5):489–498 DOI [10.1016/j.jplph.2008.07.003](https://doi.org/10.1016/j.jplph.2008.07.003).
- Mount SM, Christian BH, Gerald GD, Stormo W, Chris F. 2012. Splicing signals in Drosophila: intron size, information content, and consensus sequences. *Nucleic Acids Research* **20**(16):4255–4262 DOI [10.1093/nar/20.16.4255](https://doi.org/10.1093/nar/20.16.4255).
- Ning H, Ji XL, Du YP, Xi H, Zhao XJ, Zhai H. 2017. Identification of a novel alternative splicing variant of *VvPMA1* in grape root under salinity. *Frontiers in Plant Science* **8**:605 DOI [10.3389/fpls.2017.00605](https://doi.org/10.3389/fpls.2017.00605).
- Nomchit K, Harvey AJ, Maria H, Harry B, Ines E, Teeri T, Fincher GB. 2010. Heterologous expression of diverse barley *XTH* genes in the yeast *Pichia pastoris*. *Plant Biotechnology Journal* **27**(3):251–258 DOI [10.5511/plantbiotechnology.27.251](https://doi.org/10.5511/plantbiotechnology.27.251).
- Norbert H, Andrea G, Judit D, Jaime A. 2020. Mining sequences with similarity to *XTH* genes in the *Solanum tuberosum* L. transcriptome: introductory step for identifying homologous *XTH* genes. *Plant Signaling & Behavior* **15**(10):1797294 DOI [10.1080/15592324.2020.1797294](https://doi.org/10.1080/15592324.2020.1797294).
- Opazo MC, Lizana R, Stappung Y, Davis TM, Herrera R, Moya-Leon MA. 2017. XTHs from *Fragaria vesca*: genomic structure and transcriptomic analysis in ripening fruit and other tissues. *BMC Genomics* **18**(1):852 DOI [10.1186/s12864-017-4255-8](https://doi.org/10.1186/s12864-017-4255-8).
- Potter SC, Aurélien L, Eddy SR, Youngmi P, Rodrigo L, Finn RD. 2018. HMMER web server: 2018 update. *Nucleic Acids Research* **46**(W1):W200–W204 DOI [10.1093/nar/gky448](https://doi.org/10.1093/nar/gky448).
- Singh AP, Tripathi SK, Nath P, Sane AP. 2011. Petal abscission in rose is associated with the differential expression of two ethylene-responsive xyloglucan endotransglucosylase/hydrolase, *RbXTH1* and *RbXTH2*. *Journal of Experimental Botany* **62**(14):5091–5103 DOI [10.1093/jxb/err209](https://doi.org/10.1093/jxb/err209).
- Stratilova B, Kozmon S, Stratilova E, Hrmova M. 2020. Plant xyloglucan xyloglucosyl transferases and the cell wall structure: subtle but significant. *Molecules* **25**(23):5619 DOI [10.3390/molecules25235619](https://doi.org/10.3390/molecules25235619).
- Strohmeier M, Hrmova M, Fischer M, Harvey AJ, Fincher GB, Pleiss J. 2004. Molecular modeling of family GH16 glycoside hydrolases: potential roles for xyloglucan transglucosylases/hydrolases in cell wall modification in the poaceae. *Protein Science* **13**(12):3200–3213 DOI [10.1110/ps.04828404](https://doi.org/10.1110/ps.04828404).

- Sudhir K, Glen S, Michael L, Christina K, Koichiro T. 2018.** MEGA X: molecular evolutionary genetics analysis across computing platforms. *Molecular Biology Evolution* **35(6)**:1547–1549 DOI [10.1093/molbev/msy096](https://doi.org/10.1093/molbev/msy096).
- Tiika RJ, Wei J, Cui G, Ma Y, Yang H. 2021.** Transcriptome-wide characterization and functional analysis of Xyloglucan endo-transglycosylase/hydrolase (*XTH*) gene family of *Salicornia europaea* L. under salinity and drought stress. *BMC Plant Biology* **21(1)**:491 DOI [10.1186/s12870-021-03269-y](https://doi.org/10.1186/s12870-021-03269-y).
- Wan S, Li W, Zhu Y, Liu Z, Zhan J. 2014.** Genome-wide identification, characterization and expression analysis of the auxin response factor gene family in *Vitis vinifera*. *Plant Cell Reports* **33(8)**:1365–1375 DOI [10.1007/s00299-014-1622-7](https://doi.org/10.1007/s00299-014-1622-7).
- Xie T, Chen C, Li J, Liu C, He Y. 2018.** Genome-wide investigation of *WRKY* gene family in pineapple: evolution and expression profiles during development and stress. *BMC Genomics* **19(1)**:1–18 DOI [10.1186/s12864-018-4880-x](https://doi.org/10.1186/s12864-018-4880-x).
- Xuan Y, Zhao HF, Guo XY, Ren J, Wang Y, Lu BY. 2016.** Plant Cell Wall Remodeling Enzyme Xyloglucan Endotransglucosylase/hydrolase (*XTH*). *Chinese Agricultural Science Bulletin* **32(18)**:83–88 DOI [10.11924/j.issn.1000-6850.casb15120059](https://doi.org/10.11924/j.issn.1000-6850.casb15120059).
- Yokoyama R. 2004.** A surprising diversity and abundance of xyloglucan endotransglucosylase/hydrolases in rice classification and expression analysis. *Plant Physiology* **134(3)**:1088–1099 DOI [10.1104/pp.103.035261](https://doi.org/10.1104/pp.103.035261).
- Zhu Y, Wu N, Song W, Yin G, Qin Y, Yan Y, Hu Y. 2014.** Soybean (*Glycine max*) expansin gene superfamily origins: segmental and tandem duplication events followed by divergent selection among subfamilies. *BMC Plant Biology* **14(1)**:93 DOI [10.1186/1471-2229-14-93](https://doi.org/10.1186/1471-2229-14-93).